Study of top quark production and decays involving a tau lepton at CDF and limits on a charged Higgs boson contribution

T. Aaltonen,[21] S. Amerio,[39a,39b] D. Amidei,[31] A. Anastassov,[15,v] A. Annovi,[17] J. Antos,[12] G. Apollinari,[15] J. A. Appel,[15] T. Arisawa,[52] A. Artikov,[13] J. Asaadi,[47] W. Ashmanskas,[15] B. Auerbach,[2] A. Aurisano,[47] F. Azfar,[38] W. Badgett,[15] T. Bae,[25] A. Barbaro-Galtieri,[26] V. E. Barnes,[43] B. A. Barnett,[23] P. Barria,[41a,41c] P. Bartos,[12] M. Bauce,[39a,39b] F. Bedeschi,[41a] S. Behari,[15] G. Bellettini,[41a,41b] J. Bellinger,[54] D. Benjamin,[14] A. Beretvas,[15] A. Bhatti,[45] K. R. Bland,[5] B. Blumenfeld,[23] A. Bocci,[14] A. Bodek,[44] D. Bortoletto,[43] J. Boudreau,[42] A. Boveia,[11] L. Brigliadori,[6a,6b] C. Bromberg,[32] E. Brucken,[21] J. Budagov,[13] H. S. Budd,[44] K. Burkett,[15] G. Busetto,[39a,39b] P. Bussey,[19] P. Butti,[41a,41b] A. Buzatu,[19] A. Calamba,[10] S. Camarda,[4] M. Campanelli,[28] F. Canelli,[11,cc] B. Carls,[22] D. Carlsmith,[54] R. Carosi,[41a] S. Carrillo,[16,l] B. Casal,[9,j] M. Casarsa,[6a] A. Castro,[6a,6b] P. Catastini,[20] D. Cauz,[48a,48b,48c] V. Cavaliere,[22] M. Cavalli-Sforza,[4] A. Cerri,[26,e] L. Cerrito,[28,q] Y. C. Chen,[1] M. Chertok,[7] G. Chiarelli,[41a] G. Chlachidze,[15] K. Cho,[25] D. Chokheli,[13] A. Clark,[18] C. Clarke,[53] M. E. Convery,[15] J. Conway,[7] M. Corbo,[15,y] M. Cordelli,[17] C. A. Cox,[7] D. J. Cox,[7] M. Cremonesi,[41a] D. Cruz,[47] J. Cuevas,[9,x] R. Culbertson,[15] N. d'Ascenzo,[15,u] M. Datta,[15,ff] P. de Barbaro,[44] L. Demortier,[45] M. Deninno,[6a] M. D'Errico,[39a,39b] F. Devoto,[21] A. Di Canto,[41a,41b] B. Di Ruzza,[15,p] J. R. Dittmann,[5] S. Donati,[41a,41b] M. D'Onofrio,[27] M. Dorigo,[48a,48d] A. Driutti,[48a,48b,48c] K. Ebina,[52] R. Edgar,[31] A. Elagin,[47] R. Erbacher,[7] S. Errede,[22] B. Esham,[22] S. Farrington,[38] J. P. Fernández Ramos,[29] R. Field,[16] G. Flanagan,[15,s] R. Forrest,[7] M. Franklin,[20] J. C. Freeman,[15] H. Frisch,[11] Y. Funakoshi,[52] C. Galloni,[41a,41b] A. F. Garfinkel,[43] P. Garosi,[41a,41c] H. Gerberich,[22] E. Gerchtein,[15] S. Giagu,[46a] V. Giakoumopoulou,[3] K. Gibson,[42] C. M. Ginsburg,[15] N. Giokaris,[3] P. Giromini,[17] G. Giurgiu,[23] V. Glagolev,[13] D. Glenzinski,[15] M. Gold,[34] D. Goldin,[47] A. Golossanov,[15] G. Gomez,[9] G. Gomez-Ceballos,[30] M. Goncharov,[30] O. González López,[29] I. Gorelov,[34] A. T. Goshaw,[14] K. Goulianos,[45] E. Gramellini,[6a] S. Grinstein,[4] C. Grosso-Pilcher,[11] R. C. Group,[51,15] J. Guimaraes da Costa,[20] S. R. Hahn,[15] J. Y. Han,[44] F. Happacher,[17] K. Hara,[49] M. Hare,[50] R. F. Harr,[53] T. Harrington-Taber,[15,m] K. Hatakeyama,[5] C. Hays,[38] J. Heinrich,[40] M. Herndon,[54] A. Hocker,[15] Z. Hong,[47] W. Hopkins,[15,f] S. Hou,[1] R. E. Hughes,[35] U. Husemann,[55] M. Hussein,[32,aa] J. Huston,[32] G. Introzzi,[41a,41e,41f] M. Iori,[46a,46b] A. Ivanov,[7,o] E. James,[15] D. Jang,[10] B. Jayatilaka,[15] E. J. Jeon,[25] S. Jindariani,[15] M. Jones,[43] K. K. Joo,[25] S. Y. Jun,[10] T. R. Junk,[15] M. Kambeitz,[24] T. Kamon,[25,47] P. E. Karchin,[53] A. Kasmi,[5] Y. Kato,[37,n] W. Ketchum,[11,gg] J. Keung,[40] B. Kilminster,[15,cc] D. H. Kim,[25] H. S. Kim,[25] J. E. Kim,[25] M. J. Kim,[17] S. H. Kim,[49] S. B. Kim,[25] Y. J. Kim,[25] Y. K. Kim,[11] N. Kimura,[52] M. Kirby,[15] K. Knoepfel,[15] K. Kondo,[52,*] D. J. Kong,[25] J. Konigsberg,[16] A. V. Kotwal,[14] M. Kreps,[24] J. Kroll,[40] M. Kruse,[14] T. Kuhr,[24] M. Kurata,[49] A. T. Laasanen,[43] S. Lammel,[15] M. Lancaster,[28] K. Lannon,[35,w] G. Latino,[41a,41c] H. S. Lee,[25] J. S. Lee,[25] S. Leo,[41a] S. Leone,[41a] J. D. Lewis,[15] A. Limosani,[14,r] E. Lipeles,[40] A. Lister,[18,a] H. Liu,[51] Q. Liu,[43] T. Liu,[15] S. Lockwitz,[55] A. Loginov,[55] D. Lucchesi,[39a,39b] A. Lucà,[17] J. Lueck,[24] P. Lujan,[26] P. Lukens,[15] G. Lungu,[45] J. Lys,[26] R. Lysak,[12,d] R. Madrak,[15] P. Maestro,[41a,41c] S. Malik,[45] G. Manca,[27,b] A. Manousakis-Katsikakis,[3] L. Marchese,[6a,hh] F. Margaroli,[46a] P. Marino,[41a,41d] M. Martínez,[4] K. Matera,[22] M. E. Mattson,[53] A. Mazzacane,[15] P. Mazzanti,[6a] R. McNulty,[27,i] A. Mehta,[27] P. Mehtala,[21] C. Mesropian,[45] T. Miao,[15] D. Mietlicki,[31] A. Mitra,[1] H. Miyake,[49] S. Moed,[15] N. Moggi,[6a] C. S. Moon,[15,y] R. Moore,[15,dd,ee] M. J. Morello,[41a,41d] A. Mukherjee,[15] Th. Muller,[24] P. Murat,[15] M. Mussini,[6a,6b] J. Nachtman,[15,m] Y. Nagai,[49] J. Naganoma,[52] I. Nakano,[36] A. Napier,[50] J. Nett,[47] C. Neu,[51] T. Nigmanov,[42] L. Nodulman,[2] S. Y. Noh,[25] O. Norniella,[22] L. Oakes,[38] S. H. Oh,[14] Y. D. Oh,[25] I. Oksuzian,[51] T. Okusawa,[37] R. Orava,[21] L. Ortolan,[4] C. Pagliarone,[48a] E. Palencia,[9,e] P. Palni,[34] V. Papadimitriou,[15] W. Parker,[54] G. Pauletta,[48a,48b,48c] M. Paulini,[10] C. Paus,[30] T. J. Phillips,[14] G. Piacentino,[41a] E. Pianori,[40] J. Pilot,[7] K. Pitts,[22] C. Plager,[8] L. Pondrom,[54] S. Poprocki,[15,f] K. Potamianos,[26] A. Pranko,[26] F. Prokoshin,[13,z] F. Ptohos,[17,g] G. Punzi,[41a,41b] N. Ranjan,[43] I. Redondo Fernández,[29] P. Renton,[38] M. Rescigno,[46a] F. Rimondi,[6a,*] L. Ristori,[41,15] C. Rizzi,[15] A. Robson,[19] T. Rodriguez,[40] S. Rolli,[50,h] M. Ronzani,[41a,41b] R. Roser,[15] J. L. Rosner,[11] F. Ruffini,[41a,41c] A. Ruiz,[9] J. Russ,[10] V. Rusu,[15] W. K. Sakumoto,[44] Y. Sakurai,[52] L. Santi,[48a,48b,48c] K. Sato,[49] V. Saveliev,[15,u] A. Savoy-Navarro,[15,y] P. Schlabach,[15] E. E. Schmidt,[15] T. Schwarz,[31] L. Scodellaro,[9] F. Scuri,[41a] S. Seidel,[34] Y. Seiya,[37] A. Semenov,[13] F. Sforza,[41a,41b] S. Z. Shalhout,[7] T. Shears,[27] P. F. Shepard,[42] M. Shimojima,[49,t] M. Shochet,[11] I. Shreyber-Tecker,[33] A. Simonenko,[13] K. Sliwa,[50] J. R. Smith,[7] F. D. Snider,[15] H. Song,[42] V. Sorin,[4] R. St. Denis,[19,*] M. Stancari,[15] D. Stentz,[15,v] J. Strologas,[34] Y. Sudo,[49] A. Sukhanov,[15] I. Suslov,[13] K. Takemasa,[49] Y. Takeuchi,[49] J. Tang,[11] M. Tecchio,[31] P. K. Teng,[1] J. Thom,[15,f] E. Thomson,[40] V. Thukral,[47] D. Toback,[47] S. Tokar,[12] K. Tollefson,[32] T. Tomura,[49] D. Tonelli,[15,e] S. Torre,[17] D. Torretta,[15] P. Totaro,[39a] M. Trovato,[41a,41d] F. Ukegawa,[49] S. Uozumi,[25] G. Velev,[15] C. Vellidis,[15] C. Vernieri,[41a,41d] M. Vidal,[43] R. Vilar,[9] J. Vizán,[9,bb] M. Vogel,[34] G. Volpi,[17] F. Vázquez,[16,l] P. Wagner,[40] R. Wallny,[15,j] S. M. Wang,[1] D. Waters,[28] W. C. Wester III,[15] D. Whiteson,[40,c] A. B. Wicklund,[2] S. Wilbur,[7] H. H. Williams,[40] J. S. Wilson,[31] P. Wilson,[15] B. L. Winer,[35] P. Wittich,[15,f] S. Wolbers,[15] H. Wolfe,[35] T. Wright,[31] X. Wu,[18] Z. Wu,[5] K. Yamamoto,[37] D. Yamato,[37] T. Yang,[15] U. K. Yang,[25] Y. C. Yang,[25] W.-M. Yao,[26]

G. P. Yeh,[15] K. Yi,[15,m] J. Yoh,[15] K. Yorita,[52] T. Yoshida,[37,k] G. B. Yu,[14] I. Yu,[25] A. M. Zanetti,[48a] Y. Zeng,[14] C. Zhou,[14] and S. Zucchelli[6a,6b]

(CDF Collaboration)

[1]*Institute of Physics, Academia Sinica, Taipei, Taiwan 11529, Republic of China*
[2]*Argonne National Laboratory, Argonne, Illinois 60439, USA*
[3]*University of Athens, 157 71 Athens, Greece*
[4]*Institut de Fisica d'Altes Energies, ICREA, Universitat Autonoma de Barcelona, E-08193, Bellaterra (Barcelona), Spain*
[5]*Baylor University, Waco, Texas 76798, USA*
[6a]*Istituto Nazionale di Fisica Nucleare Bologna, I-40127 Bologna, Italy*
[6b]*University of Bologna, I-40127 Bologna, Italy*
[7]*University of California, Davis, Davis, California 95616, USA*
[8]*University of California, Los Angeles, Los Angeles, California 90024, USA*
[9]*Instituto de Fisica de Cantabria, CSIC-University of Cantabria, 39005 Santander, Spain*
[10]*Carnegie Mellon University, Pittsburgh, Pennsylvania 15213, USA*
[11]*Enrico Fermi Institute, University of Chicago, Chicago, Illinois 60637, USA*
[12]*Comenius University, 842 48 Bratislava, Slovakia;*
Institute of Experimental Physics, 040 01 Kosice, Slovakia
[13]*Joint Institute for Nuclear Research, RU-141980 Dubna, Russia*
[14]*Duke University, Durham, North Carolina 27708, USA*
[15]*Fermi National Accelerator Laboratory, Batavia, Illinois 60510, USA*
[16]*University of Florida, Gainesville, Florida 32611, USA*
[17]*Laboratori Nazionali di Frascati, Istituto Nazionale di Fisica Nucleare, I-00044 Frascati, Italy*
[18]*University of Geneva, CH-1211 Geneva 4, Switzerland*
[19]*Glasgow University, Glasgow G12 8QQ, United Kingdom*
[20]*Harvard University, Cambridge, Massachusetts 02138, USA*
[21]*Division of High Energy Physics, Department of Physics, University of Helsinki, FIN-00014, Helsinki, Finland; Helsinki Institute of Physics, FIN-00014, Helsinki, Finland*
[22]*University of Illinois, Urbana, Illinois 61801, USA*
[23]*The Johns Hopkins University, Baltimore, Maryland 21218, USA*
[24]*Institut für Experimentelle Kernphysik, Karlsruhe Institute of Technology, D-76131 Karlsruhe, Germany*
[25]*Center for High Energy Physics, Kyungpook National University, Daegu 702-701, Korea;*
Seoul National University, Seoul 151-742, Korea; Sungkyunkwan University, Suwon 440-746, Korea;
Korea Institute of Science and Technology Information, Daejeon 305-806, Korea;
Chonnam National University, Gwangju 500-757, Korea; Chonbuk National University,
Jeonju 561-756, Korea; Ewha Womans University, Seoul, 120-750, Korea
[26]*Ernest Orlando Lawrence Berkeley National Laboratory, Berkeley, California 94720, USA*
[27]*University of Liverpool, Liverpool L69 7ZE, United Kingdom*
[28]*University College London, London WC1E 6BT, United Kingdom*
[29]*Centro de Investigaciones Energeticas Medioambientales y Tecnologicas, E-28040 Madrid, Spain*
[30]*Massachusetts Institute of Technology, Cambridge, Massachusetts 02139, USA*
[31]*University of Michigan, Ann Arbor, Michigan 48109, USA*
[32]*Michigan State University, East Lansing, Michigan 48824, USA*
[33]*Institution for Theoretical and Experimental Physics, ITEP, Moscow 117259, Russia*
[34]*University of New Mexico, Albuquerque, New Mexico 87131, USA*
[35]*The Ohio State University, Columbus, Ohio 43210, USA*
[36]*Okayama University, Okayama 700-8530, Japan*
[37]*Osaka City University, Osaka 558-8585, Japan*
[38]*University of Oxford, Oxford OX1 3RH, United Kingdom*
[39a]*Istituto Nazionale di Fisica Nucleare, Sezione di Padova, I-35131 Padova, Italy*
[39b]*University of Padova, I-35131 Padova, Italy*
[40]*University of Pennsylvania, Philadelphia, Pennsylvania 19104, USA*
[41a]*Istituto Nazionale di Fisica Nucleare Pisa, I-56127 Pisa, Italy*
[41b]*University of Pisa, I-56127 Pisa, Italy*
[41c]*University of Siena, I-56127 Pisa, Italy*
[41d]*Scuola Normale Superiore, I-56127 Pisa, Italy*
[41e]*INFN Pavia, I-27100 Pavia, Italy*
[41f]*University of Pavia, I-27100 Pavia, Italy*

[42]University of Pittsburgh, Pittsburgh, Pennsylvania 15260, USA
[43]Purdue University, West Lafayette, Indiana 47907, USA
[44]University of Rochester, Rochester, New York 14627, USA
[45]The Rockefeller University, New York, New York 10065, USA
[46a]Istituto Nazionale di Fisica Nucleare, Sezione di Roma 1, I-00185 Roma, Italy
[46b]Sapienza Università di Roma, I-00185 Roma, Italy
[47]Mitchell Institute for Fundamental Physics and Astronomy, Texas A&M University,
College Station, Texas 77843, USA
[48a]Istituto Nazionale di Fisica Nucleare Trieste, I-33100 Udine, Italy
[48b]Gruppo Collegato di Udine, I-33100 Udine, Italy
[48c]University of Udine, I-33100 Udine, Italy
[48d]University of Trieste, I-34127 Trieste, Italy
[49]University of Tsukuba, Tsukuba, Ibaraki 305, Japan
[50]Tufts University, Medford, Massachusetts 02155, USA
[51]University of Virginia, Charlottesville, Virginia 22906, USA
[52]Waseda University, Tokyo 169, Japan
[53]Wayne State University, Detroit, Michigan 48201, USA
[54]University of Wisconsin, Madison, Wisconsin 53706, USA
[55]Yale University, New Haven, Connecticut 06520, USA

We present an analysis of top-antitop quark production and decay into a tau lepton, tau neutrino, and bottom quark using data from 9 fb^{-1} of integrated luminosity at the Collider Detector at Fermilab. Dilepton events, where one lepton is an energetic electron or muon and the other a hadronically decaying tau lepton, originating from proton-antiproton collisions at $\sqrt{s} = 1.96$ TeV, are used. A top-antitop quark production cross section of 8.1 ± 2.1 pb is measured, assuming standard-model top quark decays. By separately identifying for the first time the single-tau and the ditau components, we measure the branching fraction of

[*]Deceased.
[a]Visitor from University of British Columbia, Vancouver, British Columbia V6T 1Z1, Canada.
[b]Visitor from Istituto Nazionale di Fisica Nucleare, Sezione di Cagliari, 09042 Monserrato (Cagliari), Italy.
[c]Visitor from University of California Irvine, Irvine, California 92697, USA.
[d]Visitor from Institute of Physics, Academy of Sciences of the Czech Republic, 182 21, Czech Republic.
[e]Visitor from CERN, CH-1211 Geneva, Switzerland.
[f]Visitor from Cornell University, Ithaca, New York 14853, USA.
[g]Visitor from University of Cyprus, Nicosia CY-1678, Cyprus.
[h]Visitor from Office of Science, U.S. Department of Energy, Washington, D.C. 20585, USA.
[i]Visitor from University College Dublin, Dublin 4, Ireland.
[j]Visitor from ETH, 8092 Zürich, Switzerland.
[k]Visitor from University of Fukui, Fukui City, Fukui Prefecture, Japan 910-0017.
[l]Visitor from Universidad Iberoamericana, Lomas de Santa Fe, México, C.P. 01219, Distrito Federal.
[m]Visitor from University of Iowa, Iowa City, Iowa 52242, USA.
[n]Visitor from Kinki University, Higashi-Osaka City, Japan 577-8502.
[o]Visitor from Kansas State University, Manhattan, Kansas 66506, USA.
[p]Visitor from Brookhaven National Laboratory, Upton, New York 11973, USA.
[q]Visitor from Queen Mary, University of London, London, E1 4NS, United Kingdom.
[r]Visitor from University of Melbourne, Victoria 3010, Australia.
[s]Visitor from Muons, Inc., Batavia, Illinois 60510, USA.
[t]Visitor from Nagasaki Institute of Applied Science, Nagasaki 851-0193, Japan.
[u]Visitor from National Research Nuclear University, Moscow 115409, Russia.
[v]Visitor from Northwestern University, Evanston, Illinois 60208, USA.
[w]Visitor from University of Notre Dame, Notre Dame, Indiana 46556, USA.
[x]Visitor from Universidad de Oviedo, E-33007 Oviedo, Spain.
[y]Visitor from CNRS-IN2P3, Paris, F-75205 France.
[z]Visitor from Universidad Tecnica Federico Santa Maria, 110v Valparaiso, Chile.
[aa]Visitor from The University of Jordan, Amman 11942, Jordan.
[bb]Visitor from Universite catholique de Louvain, 1348 Louvain-La-Neuve, Belgium.
[cc]Visitor from University of Zürich, 8006 Zürich, Switzerland.
[dd]Visitor from Massachusetts General Hospital, Boston, Massachusetts 02114, USA.
[ee]Visitor from Harvard Medical School, Boston, Massachusetts 02114, USA.
[ff]Visitor from Hampton University, Hampton, Virginia 23668, USA.
[gg]Visitor from Los Alamos National Laboratory, Los Alamos, New Mexico 87544, USA.
[hh]Visitor from Università degli Studi di Napoli Federico I, I-80138 Napoli, Italy.

the top quark into the tau lepton, tau neutrino, and bottom quark to be $(9.6 \pm 2.8)\%$. The branching fraction of top quark decays into a charged Higgs boson and a bottom quark, which would imply violation of lepton universality, is limited to be less than 5.9% at a 95% confidence level [for $\mathcal{B}(\mathrm{H}^- \to \tau\bar{\nu}) = 1$].

The large integrated luminosity provided by the 2001–2011 operations of the Tevatron proton-antiproton collider enables the Fermilab collider detector experiments to perform precision measurements of top quark properties [1]. Within the standard model the top quark decays into a W boson and bottom quark, which is the dominant decay mode [2]. However, new particles beyond the standard model, like charged bosons, could open additional decay modes. Higgs bosons with unit electric charge are predicted by extensions of the standard model that contain an extended Higgs sector, such as two Higgs doublet models [3]. For charged Higgs bosons lighter than the top quark, one of the most interesting decay modes is into a tau lepton and neutrino, with a branching fraction close to 1 in a large region of parameter space.

This paper presents an analysis of dilepton events predominantly originated from top-antitop quark ($t\bar{t}$) production, where one of the leptons is an electron or muon and the other a hadronically decaying tau. For hadronically decaying tau leptons, both online event selection, trigger, and identification are demanding due to the relatively short lifetime of tau leptons and the presence of one or more neutrinos in the final state. We measure top production and decay properties: the $t\bar{t}$ production cross section and top branching fraction into a tau lepton, neutrino, and bottom quark. Separating top quark decays where the electron or muon originates from a tau decay from those where it originates directly from a W boson decay enables us to measure the branching fraction without relying on a theoretical cross-section calculation.

The Collider Detector at Fermilab, CDF, experiment [4] is located at the Fermilab Tevatron. The data used in the analysis presented here were collected between 2001 and 2011 at a center-of-mass energy of 1.96 TeV and correspond to an integrated luminosity of 9 fb^{-1}. Of particular importance for the analysis is the charged-particle trajectory measurement (tracking) system. It is comprised of a silicon-microstrip-detector system [5] close to the collision region and an open-cell drift chamber [6], both immersed in a 1.4 Tesla solenoidal field. They enable measuring the transverse momentum [7] of charged particles with a resolution of about 150 MeV/c at 10 GeV/c. Outside the tracking system are electromagnetic and hadronic sampling calorimeters [8] segmented in a projective-tower geometry of about 0.1 units in pseudorapidity and 15 degrees in azimuthal angle [7]. Drift chambers and scintillators are located outside the calorimeters to identify muons [9]. Events for this analysis are selected by triggers designed to collect samples enriched in decays of low-momentum tau leptons for nonstandard-model physics searches. The triggers require an electron or muon candidate with at least 8 GeV/c and a charged particle of at least 5 GeV/c of transverse momentum. In the later part of the data taking, triggers also require the track to point to a narrow energy deposition of 5 GeV or more in five or fewer calorimeter towers, thus requiring a more taulike signature.

At the Tevatron, $t\bar{t}$ production via quark-antiquark annihilation is the dominant top quark production process. Top dilepton events with one hadronic tau decay have two sources: (i) events with one top quark decaying into an electron or muon, neutrino, and bottom quark and the other into a tau lepton, neutrino, and bottom quark ("single tau"); and (ii) events with both top quarks decaying into a tau lepton, neutrino, and bottom quark and one tau decaying leptonically and the other hadronically ("ditau"). The neutrinos escape direct detection and result in a momentum imbalance in the event. The bottom quarks are each identified as a cluster of hadronic energy, jet, with a displaced secondary vertex, from the long-lived bottom quark hadrons.

After event reconstruction [4], we select events with one central, isolated electron or muon candidate of 10 GeV/c or higher that meets standard CDF identification requirements [10] and one central, isolated, one-prong or three-prong tau candidate [11] with transverse momentum $p_T \geq 15$ and 20 GeV/c, respectively. The reconstruction and identification of a hadronic tau decay starts with a calorimeter tower of transverse energy $E_T \geq 6$ GeV [7] and a charged particle of $p_T \geq 6$ GeV/c pointing to it. Neighboring towers with 1 GeV or more of transverse energy are added. Since tau decays yield highly collimated jets, calorimeter clusters with more than six towers are rejected. A signal cone with aperture 2ϑ is defined around the track. Its size $\vartheta = \min(0.17, 5.0 \text{ GeV}/E)$ depends on the calorimeter-cluster energy E; i.e. it shrinks for cluster energies above 30 GeV. Charged particles with $p_T \geq 1$ GeV/c within the cone are associated with the tau candidate and define its track multiplicity or number of prongs. For one-prong tau candidates, the calorimeter cluster is required to have $E_T \geq 10$ GeV and for three-prong candidates $E_T \geq 15$ GeV. To suppress contamination from minimum ionizing particles in the calorimeter, the E_T of the calorimeter cluster should be at least 40% of the scalar sum of the transverse momenta of charged particles in the signal cone. An isolation annulus between the signal cone and $\pi/6$ is used to further suppress quark and gluon jets. No charged particle with $p_T \geq 1.5$ GeV/c or neutral pion candidate [12] is allowed in this region and the scalar transverse momentum sum of the charged

particles inside the region must not exceed 2 GeV/c. To suppress electron contamination, tau candidates associated with very small energy in the hadronic calorimeter compared to the transverse momentum sum of the charged particles are rejected [13]. The four-momentum vector of the tau candidate is calculated from the charged particles and neutral pions inside the signal cone. Since the tau decay produces a neutrino, the reconstructed mass should be smaller than the mass of the tau lepton and it is thus required to be less than 1.8 GeV/c^2. Tau candidates whose three final-state charged particles have the same electric charge are rejected as are events where the charge of the tau candidate and of the electron or muon candidate have the same sign.

Identified Z^0 decays and low-mass muon pairs from the Drell-Yan process are removed with dilepton mass requirements. If the two-body mass of the electron plus any calorimeter cluster with over 90% of energy in the electromagnetic compartment falls within the range of 86 to 96 GeV/c^2, the event is rejected. Similarly, if the two-body mass of the muon and any minimum ionizing particle falls within the range of 76 to 106 GeV/c^2 or is below 15 GeV/c^2 the event is rejected.

For the identification of bottom quark jets, we use the SECVTX tagger [14] to identify secondary vertices within a jet that are displaced from the primary interaction vertex of the event. We require two jets [15], one with $E_T >$ 20 GeV and a second with $E_T > 15$ GeV, both within $|\eta| \leq 2$ [7]. At least one jet should be tagged as a candidate for containing a long-lived bottom quark hadron; i.e., it has a secondary vertex with a decay length in the transverse plane that exceeds three times its uncertainty. The efficiency of the SECVTX tagger is about 44% for bottom quark jets in the central region with about a 1% mistag rate for light quark and gluon jets.

Events from $t\bar{t}$ production with leptonic W decays and one hadronic tau decay have three or five neutrinos in the final state (not counting possible semileptonic heavy quark decays). The sum of the transverse momenta of the neutrinos is measured by the missing transverse energy E_T [16] of the event. Events are required to have $E_T \geq 10$ GeV, a small amount compared to other $t\bar{t}$ analyses [1] with one (or two) neutrinos from a W decay in the final state.

To purify the selection of $t\bar{t}$ events we exploit the large top quark mass and require events to have a large amount of transverse energy in the final state: $H_T = E_T + E_T^{tau} + \sum E_T^{jet} \geq 150$ GeV (≥ 155 GeV in the case of three-prong tau candidates). Contrary to other top quark analyses [1], the E_T of the electron or muon is not included in H_T. The electron or muon can come from either top or tau decay and including its E_T in the H_T would favor single-tau (with a more energetic electron or muon) over ditau events in the selection. This selection defines the initial analysis sample.

To study background sources and the signal we generate events using the ALPGEN and PYTHIA Monte Carlo

programs [17], using a top quark mass of 173 GeV/c^2. To mimic geometrical and kinematical acceptances, the generated events are passed through a GEANT-based detector simulation [14]. Event yields are normalized using theoretical next-to-leading-order cross-section calculations [18] and scaled for trigger efficiencies and any differences in lepton identification efficiencies between data and simulated events.

To estimate the background contribution from quark and gluon jets misidentified as hadronic tau decays, events triggered on single jets or on single electrons or muons are used. First, the probability of a hadronic jet to be misidentified as a tau lepton is measured. In the second step, this probability is used to weight the jets in events with an electron or muon candidate to estimate and study the misidentified-tau-lepton contribution in our electron-or-muon-plus-tau sample. Signal events are naturally excluded in this method due to the exclusive one-tau-candidate selection in the initial analysis sample.

For the misidentification-probability measurement, we use jet-triggered data with calorimeter jet-E_T thresholds of 5 to 100 GeV. The trigger bias is removed by requiring at least two jets in each event to pass the trigger requirements. For the probability calculation we use taulike jets, i.e., calorimeter jets that pass the tau identification requirements above except for the isolation and mass requirements. There is a small contribution from genuine tau-lepton decays in the jet sample due to vector boson (and top quark) decays involving a tau. This contribution is suppressed by requiring the jet events to have insignificant missing transverse energy [20] and no identified electron or muon with $E_T > 10$ GeV. Leading and subleading jets have different proportions of gluons and quarks resulting in different probabilities for tau misidentification. We treat these jets separately, average their misidentification rates to determine the nominal tau-misidentification probability, and use the difference to each as a measure of the systematic uncertainty. The probability is parametrized as a function of jet E_T, η, and number of prongs. Probabilities range from 1% to 10% per taulike jet or 0.1% to 1% per generic jet. The measurement of the tau-misidentification probability is checked in two control regions, a multijet and a W plus jet enriched sample.

To estimate the contribution of jets misidentified as tau candidates in this analysis, single-lepton-triggered data are used. CDF recorded events requiring only a $p_T > 8$ GeV/c electron or muon candidate. For each taulike jet in those events, we mimic a tau candidate with the above measured probability, correct for the difference in sample size with respect to the signal sample, and analyze it analogously to the signal sample. With this approach we simulate event characteristics, study the contribution of events with a misidentified tau lepton, and properly apply kinematic selections to reduce this background.

In the initial analysis sample we observe 58 events with an expectation of about 34 $t\bar{t}$ dilepton events [19] and about

4 events from Drell-Yan and diboson production. Astoundingly, the calculation of misidentified tau leptons shows a contribution of approximately 16 events. We find over half of them to be $t\bar{t}$ events, but with one of the top quarks decaying leptonically and the other hadronically. Four jets provide the occasion to be misidentified as a tau lepton, while the rest of the event satisfies the selection with effectively the same efficiency as the signal. To reject this background, a likelihood function $\mathcal{L}_1$ is constructed based on two tau identification variables and three kinematic variables to distinguish single-lepton from dilepton-$t\bar{t}$ events: (i) the ratio of tau-calorimeter cluster E_T to a signal-cone-charged-particle-p_T sum is used in the tau identification to reject the muon background. Compared to genuine tau leptons the distribution of this ratio for jets misidentified as taus is broader with a long tail. (ii) The charged-particle p_T sum in the isolation annulus is required to be less than 2 GeV/c in the tau candidate selection. It provides further discrimination as tau leptons in top quark decays are isolated, while jets misidentified as taus have a nearly uniform distribution within the remaining phase space. (iii) The one neutrino in the single-lepton $t\bar{t}$ events yields a E_T of around half the W boson mass and (iv) a transverse mass of electron or muon plus missing E_T up to the W mass. (v) Events with a hadronic top quark decay have an extra jet. One of the two extra jets in the event must be misidentified as a tau lepton. The jet may not be reconstructed, and dilepton $t\bar{t}$ events may have additional jets from initial- or final-state radiation. The E_T of any third jet becomes the final variable for the likelihood. Figure 1 shows the distribution of the likelihood function for data compared to the expectation from top dilepton, Drell-Yan, diboson, and misidentified tau lepton events. A $\log \mathcal{L}_1 > 0$ requirement leaves 36 events in the data with 26.7 ± 3.4 $t\bar{t}$ dilepton events, 3.1 ± 0.5 Drell-Yan and diboson events, and 4.0 ± 1.1 events expected from jets misidentified as tau leptons.
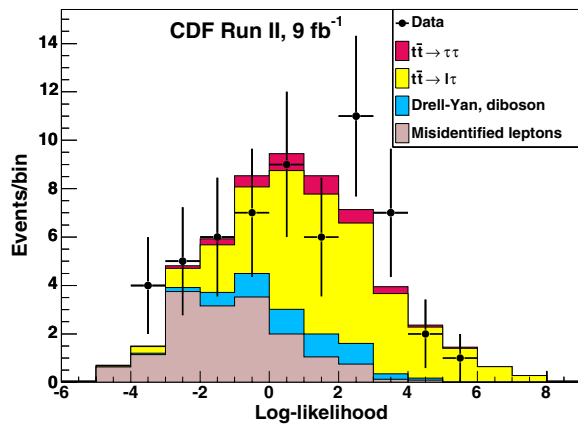

FIG. 1 (color online).   Log-likelihood $\mathcal{L}_1$ distribution for data, top dilepton, Drell-Yan plus diboson production, and misidentified lepton events.

Assuming a standard-model top quark decay, i.e., a branching fraction $\mathcal{B}(t \to W^+ b) = 1$, an acceptance corrected $t\bar{t}$ production cross section of $8.1 \pm 1.7(\text{stat})^{+1.2}_{-1.1}(\text{syst}) \pm 0.5(\text{lumi})$ pb is measured. Acceptance corrections are based on leading-order parton shower Monte Carlo simulations and the CDF detector simulation described above. Branching fractions for both W boson and tau lepton decays are taken from [2]. Lepton, jet, and bottom-quark-tagging efficiencies are estimated previously [1,10,11,14]. The systematic uncertainties include experimental contributions from lepton acceptance and identification, trigger efficiency, tau- and jet-energy-scale corrections, tagging efficiency ($\pm 5\%$), mistag rate ($\pm 20\%$), tau-misidentification probability ($^{+7\%}_{-20\%}$) [20], modeling of additional collisions contained in an event, pileup, measurement of the integrated luminosity ($\pm 5.9\%$) and theoretical contributions from the cross section of Drell-Yan and diboson production, choice of parton distribution functions, color reconnection, initial- and final-state radiation ($\pm 9\%$), fragmentation and parton showering. The uncertainty of the dominant systematic effects are provided in parentheses (which is not their contribution to the cross-section uncertainty). This cross-section measurement in the ditau channel complements the more precise measurements in the electron, muon and hadronic channels [1].

Using the theoretical $t\bar{t}$ production cross section instead of the standard-model decay branching fractions, we can extract a branching fraction of the top quark decay into a tau lepton, tau neutrino, and bottom quark. However, the data sample contains two $t\bar{t}$ components: a single-tau component that is proportional to the top quark into the tau lepton, tau neutrino, and bottom quark branching fraction (times the top quark into the electron or muon, neutrino, and bottom quark branching fraction) and a ditau component that is proportional to the branching fraction squared. Separating the two components allows measurement of the top quark into the tau, neutrino, and bottom quark branching fraction (and the $t\bar{t}$ production cross section) directly without theoretical assumption on either. For this, a second likelihood, $\mathcal{L}_2$, is constructed using the following three variables. The leptonic tau decay yields two neutrinos close to the electron or muon direction, in addition to the neutrino from the W decay. (i) This impacts the distribution of transverse mass [7] of the electron or muon plus missing E_T (Fig. 2) and (ii) the distribution of the azimuthal angle between electron or muon and missing E_T (Fig. 3). (iii) It also leads to, on average, lower p_T of electrons or muons in ditau events, as shown in Fig. 4. The ditau component contributes more at large $\mathcal{L}_2$ while the single-tau component is shifted toward smaller values of $\mathcal{L}_2$, as shown in Fig. 5.

We use the MClimit [21] package to fit the likelihood distribution with a single-tau component that has a linear dependence on the branching fraction of a top quark into a tau, neutrino, and bottom quark, and a ditau component that
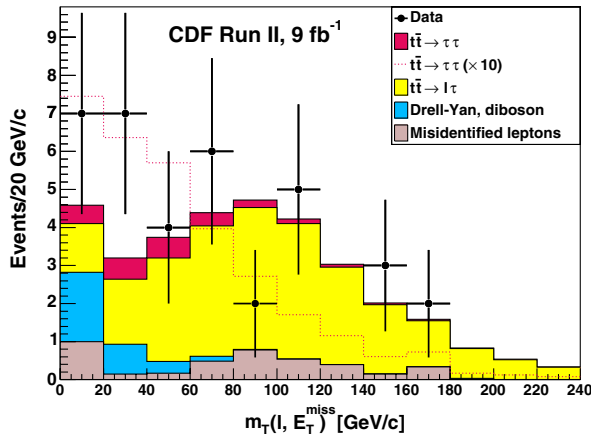
FIG. 2 (color online). Transverse mass distribution of the electron or muon plus missing E_T for data, single-tau $t\bar{t}$, ditau $t\bar{t}$, and non-$t\bar{t}$ events. For the purpose of comparing the single-tau and ditau shapes, used in the likelihood, a line shows the ditau contribution scaled to the number of single-tau events and plotted on top of the background.

has a quadratic branching-fraction dependence. The expected background contributions from Drell-Yan, diboson production, and jets misidentified as tau leptons are included in the fit and allowed to vary within their uncertainties. The systematic uncertainties on the event yield are included via nuisance parameters. We check the effect of the largest systematic uncertainty (from the probability distribution of jets being misidentified as tau leptons) on the shape of the likelihood distribution and found it to be small. For the most precise result we make use of a third branching-fraction dependency by including the $t\bar{t}$ production cross section measured by CDF in the single-lepton channel with its uncertainty [22] as a constraint in the χ^2 fit [23] and obtain
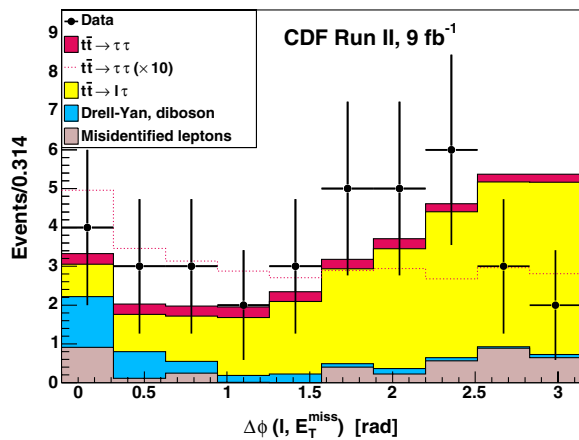

FIG. 3 (color online). Distribution of the azimuthal angle between electron or muon and missing E_T for data, single-tau $t\bar{t}$, ditau $t\bar{t}$, and non-$t\bar{t}$ events. For the purpose of comparing the single-tau and ditau shapes, used in the likelihood, a line shows the ditau contribution scaled to the number of single-tau events and plotted on top of the background.

FIG. 4 (color online). Transverse momentum distribution of the electron or muon for data, single-tau $t\bar{t}$, ditau $t\bar{t}$, and non-$t\bar{t}$ events. For the purpose of comparing the single-tau and ditau shapes, used in the likelihood, a line shows the ditau contribution scaled to the number of single-tau events and plotted on top of the background.
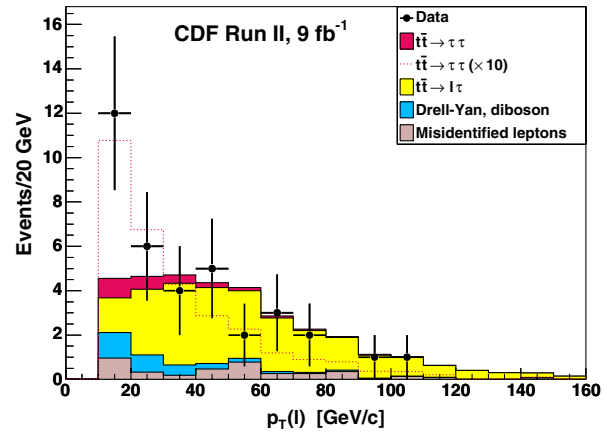
$$\mathcal{B}(t \to \tau\nu b) = 0.096 \pm 0.028,$$

with a single-tau component of 22.7 events and ditau component of 3.1 events (Fig. 5). The ratio of leptonic top branching ratios can be derived from this, and we find $\mathcal{B}(t \to \tau\nu b)/((\mathcal{B}(t \to e\nu b) + \mathcal{B}(t \to \mu\nu b))/2) = 0.88 \pm 0.26$, confirming lepton universality in top quark decays.

At a 95% confidence level the fit excludes a branching fraction of 15.8% or more of top quarks decaying into tau lepton, tau neutrino, and bottom quark (using the likelihood-ratio method [2]). A previous CDF analysis [24] found the acceptance for $t\bar{t}$ tau events with decay via a charged Higgs boson to be equal to the acceptance of events with decay via a W boson for charged Higgs masses between 80 and 140 GeV/c^2. Assuming that the top quark decays only into W and charged Higgs bosons and $\mathcal{B}(H^- \to \tau\bar{\nu}) = 1$, we exclude branching fractions for top
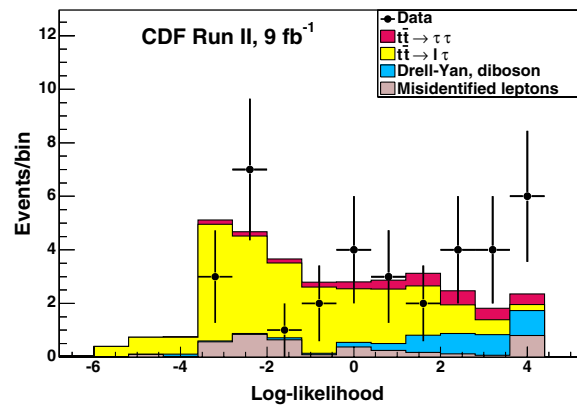

FIG. 5 (color online). Log-likelihood $\mathcal{L}_2$ distribution for data, top dilepton, Drell-Yan plus diboson production, and misidentified lepton events as determined by the fit.

T. AALTONEN *et al.* PHYSICAL REVIEW D **89,** 091101(R) (2014)

quark decays into a charged Higgs boson and a bottom quark of 5.9% or more at a 95% confidence level using the likelihood-ratio ordering [25].

With the discovery of a neutral Higgs boson at 125 GeV/c^2 by the ATLAS and CMS experiments [26], the question of an extended Higgs sector gains interest. Previous searches for a charged Higgs boson at LEP constrained its mass to be $m_{\mathrm{H}^\pm} > 78.6$ GeV/c^2 [27] and at the Tevatron constrained the branching fractions to be $\mathcal{B}(\mathrm{t} \to \mathrm{H}^+\mathrm{b}) < 0.15 - 0.19$ [for $\mathcal{B}(\mathrm{H}^- \to \tau\bar{\nu}) = 1$] and $\mathcal{B}(\mathrm{t} \to \mathrm{H}^+\mathrm{b}) < 0.10 - 0.30$ [for $\mathcal{B}(\mathrm{H}^+ \to \mathrm{c}\bar{\mathrm{s}}) = 1$] [28]. Recent LHC searches improved the limits to $\mathcal{B}(\mathrm{t} \to \mathrm{H}^+\mathrm{b}) < 0.01 - 0.05$ [29] and $< 0.02 - 0.03$ [30] for $\mathcal{B}(\mathrm{H}^- \to \tau\bar{\nu}) = 1$.

In summary, we present an analysis of dilepton $\mathrm{t}\bar{\mathrm{t}}$ events using 9 fb^{-1} of integrated luminosity at CDF. The analysis separates the single and ditau components for the first time, measuring the branching fraction of the top quark decay into a tau lepton, tau neutrino, and bottom quark at $(9.6 \pm 2.8)\%$, and testing lepton universality of the decay. The limit on the branching fraction of the top quark into a charged Higgs boson and bottom quark is comparable with recent measurements in proton-proton collisions [29,30].

[1] T. Aaltonen *et al.* (CDF and D0 Collaborations), Phys. Rev. D **86**, 092003 (2012); Phys. Rev. D **85**, 071106 (2012); T. Aaltonen *et al.* (CDF Collaboration), Phys. Lett. B **722**, 48 (2013); Phys. Rev. Lett. **106**, 161801 (2011); Phys. Rev. D **83**, 112003 (2011); Phys. Rev. Lett. **105**, 232003 (2010); Phys. Rev. D **79**, 031101 (2009); D. Acosta *et al.* (CDF Collaboration), Phys. Rev. Lett. **95**, 102002 (2005); V. M. Abazov *et al.* (D0 Collaboration), Phys. Rev. D **87**, 011103 (2013); Phys. Lett. B **713**, 165 (2012); Phys. Rev. D **85**, 091104 (2012); Phys. Rev. Lett. **108**, 032004 (2012); Phys. Rev. D **84**, 112005 (2011); Phys. Rev. Lett. **107**, 121802 (2011).

[2] J. Beringer *et al.* (Particle Data Group), Phys. Rev. D **86**, 010001 (2012). The top quark review is on page 668. The statistics review is on page 390.

[3] T. D. Lee, Phys. Rev. D **8**, 1226 (1973); J. F. Donoghue and L. F. Li, Phys. Rev. D **19**, 945 (1979); V. D. Barger, J. L. Hewett, and R. J. N. Phillips, Phys. Rev. D **41**, 3421 (1990).

[4] D. Acosta *et al.* (CDF Collaboration), Phys. Rev. D **71**, 032001 (2005).

[5] A. Sill, Nucl. Instrum. Methods Phys. Res., Sect. A **447**, 1 (2000); T. Affolder *et al.*, Nucl. Instrum. Methods Phys. Res., Sect. A **453**, 84 (2000); C. S. Hill, Nucl. Instrum. Methods Phys. Res., Sect. A **511**, 118 (2003).

[6] T. Affolder *et al.*, Nucl. Instrum. Methods Phys. Res., Sect. A **526**, 249 (2004).

[7] CDF uses a right-handed coordinate system with the origin at the nominal interaction point. θ and ϕ are the polar and azimuthal angles, defined with respect to the z axis, the proton beam direction. The transverse momentum of a particle is $p_{\mathrm{T}} = p \sin(\theta)$ and the pseudorapidity $\eta = -\ln \tan(\theta/2)$, and similarly for the transverse energy, E_{T}. The transverse mass of two particles is calculated as $m_{\mathrm{T}} = \sqrt{2E_{\mathrm{T}}^1 E_{\mathrm{T}}^2(1 - \cos(\phi^1 - \phi^2))}$.

[8] L. Balka *et al.*, Nucl. Instrum. Methods Phys. Res., Sect. A **267**, 272 (1988); S. Bertolucci *et al.*, Nucl. Instrum. Methods Phys. Res., Sect. A **267**, 301 (1988); M. Albrow *et al.*, Nucl. Instrum. Methods Phys. Res., Sect. A **480**, 524 (2002); G. Apollinari, K. Goulianos, P. Melese, and M. Lindgren, Nucl. Instrum. Methods Phys. Res., Sect. A **412**, 515 (1998).

[9] G. Ascoli, L. E. Holloway, I. Karliner, U. E. Kruse, R. D. Sard, V. J. Simaitis, D. A. Smith, and T. K. Westhusing, Nucl. Instrum. Methods Phys. Res., Sect. A **268**, 33 (1988).

[10] D. Acosta *et al.* (CDF Collaboration), Phys. Rev. Lett. **94**, 091803 (2005); A. Abulencia *et al.* (CDF Collaboration), J. Phys. G **34**, 2457 (2007).

[11] A. Abulencia *et al.* (CDF Collaboration), Phys. Rev. D **75**, 092004 (2007); D. Acosta *et al.* (CDF Collaboration), Phys. Rev. Lett. **95**, 131801 (2005).

[12] Neutral pion candidates are energy deposits in the electromagnetic calorimeter and are not reconstructed by two photons at the π^0 mass.

[13] For best electron and muon rejection, the fraction of energy in the electromagnetic compartment of the calorimeter is actually compared to the ratio of calorimeter energy and momentum sum of the charged particles in the signal cone, $(E/\sum |\vec{p}|)(0.95 - E^{\mathrm{em}}/E) > 0.1$.

[14] D. Acosta *et al.* (CDF Collaboration), Phys. Rev. D **71**, 052003 (2005).

[15] G. C. Blazey *et al.*, arXiv:hep-ex/0005012. A cone radius of 0.4 is used in the analysis presented here. A. Bhatti *et al.*, Nucl. Instrum. Methods Phys. Res., Sect. A **566**, 375 (2006). We include corrections to align the electromagnetic energy scale to the Z^0 mass, η-dependent corrections, corrections for multiple collisions in a bunch crossing and an "absolute jet energy scale" correction based on Monte Carlo simulations of particle response, multiplicity, and spectrum.

[16] While a proton and antiproton have equal but opposite momenta, the interacting partons likely have different momenta. Therefore the interaction has an unknown longitudinal boost. The missing transverse energy is defined as the opposite of the transverse component of the vector sum of the energy in the calorimeters' towers. We use E_T to denote the scalar magnitude of the missing E_T. The energy of identified minimum-ionizing particles (muons) is included in the missing E_T calculation and the energy of jets is corrected for the calorimeter response and absolute scaling.

[17] M. L. Mangano, F. Piccinini, A. D Polosa, M. Moretti, and R. Pittau, J. High Energy Phys. 07 (2003) 001; T. Sjöstrand, S. Mrenna, and P. Skands, J. High Energy Phys. 05 (2006) 026.

[18] J. Ohnemus, Phys. Rev. D **44**, 3477 (1991); S. Frixione, P. Nason, and G. Ridolfi, Nucl. Phys. **B383**, 3 (1992); J. M. Campbell and R. K. Ellis, Phys. Rev. D **60**, 113006 (1999). For Z^0/Drell-Yan plus jet production the next-to-leading-order cross sections are computed using the MCFM program. J. Campbell and R. K. Ellis, Phys. Rev. D **65**, 113007 (2002).

[19] For the expected number of $t\bar{t}$ events, a top quark mass of $m_t = 173$ GeV/c^2 and cross section of $\sigma_{t\bar{t}} = 7.5$ pb are used.

[20] CDF Collaboration, Measurement of the top pair cross section in dileptonic channels with a hadronic tau and branching fraction t → τνb, with 9.0 fb^{-1}, http://www-cdf.fnal.gov/physics/new/top/2012/ttbar_taulep_xsec_9invfb/cdf10915_TopPairDilepTau.pdf.

[21] T. Aaltonen *et al.* (CDF and D0 Collaborations), Phys. Rev. D **82**, 112005 (2010); T. Junk, Nucl. Instrum. Methods Phys. Res., Sect. A **434**, 435 (1999).

[22] T. Aaltonen *et al.* (CDF Collaborations), Phys. Rev. Lett. **105**, 012001 (2010).

[23] The cross-section measurement in the single-lepton channel has a branching-fraction dependence of $\mathcal{B}^{SM}(\text{t} \to \text{e}\nu\text{b}) \times [1 + (\mathcal{B}^{SM}(\text{t} \to \tau\nu\text{b}) - \mathcal{B}^{fit}(\text{t} \to \tau\nu\text{b}))/(1 - \mathcal{B}^{SM}(\text{t} \to \tau\nu\text{b}))]$, which is used in the fit.

[24] A. Abulencia *et al.* (CDF Collaboration), Phys. Rev. Lett. **96**, 042003 (2006).

[25] G. Feldman and R. Cousins, Phys. Rev. D **57**, 3873 (1998).

[26] G. Aad *et al.* (ATLAS Collaboration), Phys. Lett. B **716**, 1 (2012); S. Chatrchyan *et al.* (CMS Collaboration), Phys. Lett. B **716**, 30 (2012).

[27] ALEPH, DELPHI, L3 and OPAL Collaborations, The LEP Working Group for Higgs Boson Searches, arXiv:hep-ex/0107031.

[28] V. M. Abazov *et al.* (D0 Collaboration), Phys. Lett. B **682**, 278 (2009); T. Aaltonen *et al.* (CDF Collaboration), Phys. Rev. Lett. **103**, 101803 (2009).

[29] G. Aad *et al.* (ATLAS Collaboration), J. High Energy Phys. 06 (2012) 039.

[30] S. Chatrchyan *et al.* (CMS Collaboration), J. High Energy Phys. 07 (2012) 143.